EMITTANCE GROWTHS IN RESONANCE CROSSING AT FFAGS

K.Y. Ng[*], Fermilab[†], P.O. Box 500, Batavia, IL 60510

X. Pang, F. Wang, X. Wang, S.Y. Lee, Indiana University, Bloomington, IN 47405

Abstract

Scaling laws of the emittance growth for a beam crossing the 6th-order systematic space-charge resonances and the random-octupole driven 4th-order resonance are obtained by numerical multi-particle simulations. These laws can be important in setting the minimum acceleration rate and maximum tolerable resonance strength for the design of non-scaling fixed-field alternating gradient accelerators.

INTRODUCTION

Recently, fixed-field alternating gradient accelerator (FFAG) [1] has been considered as a favorable candidate for proton drivers, because it has the merit of constant guide field so that the repetition rate can be made considerably higher than conventional synchrotrons, even up to the kHzs. This is especially true for the *non-scaling design* [2], where the magnetic fields are linear and the magnet aperture need not be too large. However, the non-scaling design has the disadvantage that the betatron tunes are left to vary as the beam energy increases. Take for example, the three concentric FFAGs suggested by Ruggiero [3] to replace the Brookhaven AGS so as to reach a final beam power of more than 10 MW. Although the beam closed orbit of each FFAG has a radial excursion of less than 18 cm during the acceleration cycle, the betatron tunes vary from $\nu_{x,z} = 40.0/38.1$ to $19.1/9.3$. As shown in Fig. 1, both the systematic 4th and 6th-order resonances $m\nu_x + n\nu_z = P$ ($|m| + |n| = 4$ or 6 and $P = 136$ is the lattice periodicity) are crossed and the beam quality can become an important issue depending on the tune-ramp rate. The latter is approximately given by $\Delta\nu_{x,z}/\Delta n \sim -(1 - D/R)(\nu_{x,z}/2\beta^2 E)(\Delta E/\Delta n)$, which is typically $\sim -10^{-3}$ to -10^{-2}, where D/R is the ratio of dispersion function to the ring's radius and $\Delta E/\Delta n$ is the energy gain per revolution.
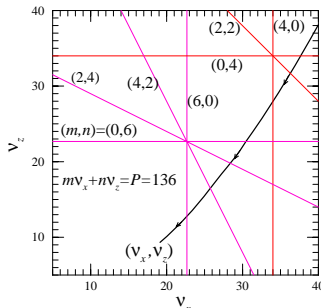
Figure 1: (Color) Tune diagram of Ruggiero's proposed FFAGs, showing the crossing of the systematic 4th and 6th-order resonances in a ramp cycle (arrowed curve).

Recently, Lee *et al*. pointed out that the crossing of space-charge driven systematic nonlinear resonances may cause substantial emittance growth [4]. He demonstrated a simple scaling property for the emittance growth across the

---

4th-order space-charge resonance. They show that random-error driven parametric linear and nonlinear resonances may also lead to emittance growth depending on how fast these resonances are crossed. The purpose of this paper is to continue the investigation of the systematic 6th-order resonances as well as the parametric 4th-order resonances, hoping to obtain the minimum resonance crossing rates so that emittance growth remains tolerable. A detailed account of this work is given in Ref. [5].

THE MODEL

Multi-particle simulations are performed on a lattice similar to that of the Fermilab Booster, which consists of $P = 24$ superperiod FODO-cells. The betatron functions are $\beta_{x,z} = 40/8.3$ m and $6.3/21.4$ m, respectively, at the centers of the F- and D-magnet sets. Four-by-four transfer matrices are employed for each half period. The transverse distribution is assumed to be bi-Gaussian all the time. Although not self-consistent, the assumption simplifies the space-charge force and speeds up the simulations tremendously. At the end of each turn, the transverse rms beam radii $\sigma_{x,z}$ and the position of the beam center are computed, and the rms emittances are inferred. These informations are used to determine the space-charge force to be applied at each F- and D-magnet set in the succeeding turn. This procedure smoothes out the computational noise in one turn, so that the number of macro-particles in the simulation, usually 2000, need not be too large.

Since the emittance usually grows much faster than a synchrotron oscillation, the performance of only 2D simulation for a slice of the beam at the longitudinal bunch center is justified. For a beam with peak linear particle density λ_b, the transverse 2D space-charge potential is

$$V_{sc}(x, z) = \frac{K_{sc}}{2} \int_0^\infty \frac{\exp\left[-\frac{x^2}{2\sigma_x^2 + t} - \frac{z^2}{2\sigma_z^2 + t}\right] - 1}{\sqrt{(2\sigma_x^2 + t)(2\sigma_z^2 + t)}} \, dt,$$

where $K_{sc} = 2\lambda_b r_0/(\beta^2\gamma^3)$ is the space-charge perveance, with r_0 being the particle classical radius and β and γ the relativistic parameters. Each beam particle passing through a magnet set experiences a horizontal space-charge kick

$$\Delta x' = -\frac{\partial V_{sc}}{\partial x}\ell = \frac{K_{sc}x\ell}{\sigma_x(\sigma_x + \sigma_z)}\exp\left[-\frac{x^2 + z^2}{(\sigma_x + \sigma_z)^2}\right],$$

and a similar vertical kick, where $\ell = \pi R/P$. Here an effective space-charge force is chosen instead, because direct derivatives of the above analytic expression is cumbersome as an apparent singularity is present whenever $\sigma_x = \sigma_z$. This effective space-charge force reproduces exactly the linear and quadrupole parts in the round-beam geometry, and rolls off far away from the beam center. Unfortunately, this effective force is not derivable from a potential. For this reason resonances that involve the mixing of the horizontal and vertical phase spaces are not addressed here.

SYSTEMATIC 6TH-ORDER RESONANCE

The beam is injected first for 100 turns at 2×10^{11} protons per turn into 84 consecutive buckets with bunching factor $B = 0.25$ and initial equal transverse normalized rms emittances $\epsilon_{N,\mathrm{rms}} = 8.33 \, \pi$mm-mr. The kinetic energy is kept constant at 1 GeV, while the betatron bare tunes initially at $\nu_{x0,z0} = 4.25/4.30$ are allowed to ramp according to some specific rate. The emittances at the end are computed and are divided by the initial to arrive at the *emittance growth factors* (EGFs). In order to minimize all other influence to the space-charge driven systematic resonances, random field errors and nonlinear fields in the magnets are turned off. Momentum width consideration is also excluded.

The terms in the space-charge potential, responsible for the 6th-order resonances can be expressed in terms of action-angle variables $(J_{x,z}, \psi_{x,z})$: $RV_{sc} \approx -\sum_{\ell}[|G_{60\ell}|J_x^3 \cos(6\psi_x - \ell\theta + \chi_{60\ell}) + |G_{06\ell}|J_z^3 \cos(6\psi_z - \ell\theta + \chi_{06\ell}) + \cdots]$, where ℓ is an integer, $|G_{mn\ell}|$ and $\chi_{mn\ell}$ are the amplitude and phase of the resonance strength. For simulation with equal horizontal and vertical emittances to start with, the space-charge contribution to the resonance strength can be factored out leaving behind the lattice dependent dimensionless reduced resonance strength $g_{mn\ell} = 4G_{mn\ell}\epsilon_{\mathrm{rms}}^3/R$, with ϵ_{rms} being the unnormalized rms emittance. Here, $K_{sc}R/(4\epsilon_{\mathrm{rms}})$ is just the linear Laslett space-charge tune shift for a round-beam geometry.

Figure 2 shows a sample tracking with 100-turn injection and tune-ramp rate -0.004 per turn. The space-charge tune shifts after injection are $\Delta\nu_{sc,x,z} = 0.309/0.290$. The systematic resonances $6\nu_{x0,z0} = P$ ($P = 24$, the lattice periodicity) are crossed at turns 950 and 825, respectively, with reduced resonance strengths $|g_{60P}|/|g_{60P}| = 0.00618/0.00463$. Both the horizontal and vertical emittances start to grow ~ 150 turns earlier. The beam size increases and the space-charge tune shifts are reduced. The right plots show the particle distribution in the vertical (bottom) and horizontal (top) phase spaces at turn 900. Six is-
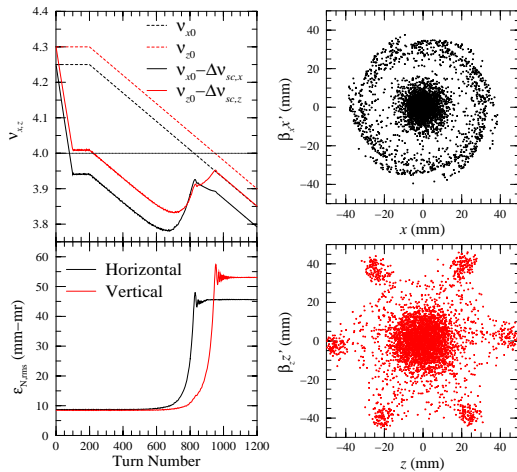
Figure 2: (Color) Top-left: After 100-turn injection, bare tunes are ramped downwards at -0.004 per turn. Systematic resonances $6\nu_{x0,z0} = P$ are crossed at turns 950 and 825, respectively. Bottom-left: Emittance growths are observed. Right: Horizontal and vertical phase-space distributions at turn 900.
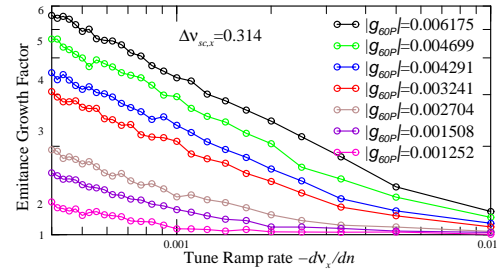
Figure 3: (Color) Emittance growth factor across the 6th-order systematic resonance $6\nu_{x0} = P$ versus tune-ramp rate for various resonance strengths $|g_{60P}|$ at 100-turn injection.

lands are clearly seen in the bottom plot slightly ahead of turn 950 when $6\nu_{z0} = P$ is crossed, and particles pushed outwards forming an outside ring encircling the inside core are seen in top plot just after crossing $6\nu_{x0} = P$.

The simulations are repeated with tune-ramp rate increasing gradually from $-d\nu_{x0,z0}/dn = 0.0004$ to 0.001. For each tune-ramp rate, the resonance strengths are also varied by assigning different values of betatron functions at the space-charge kicks. The results for 100-turn injection with EGF versus tune-ramp rate are depicted in Fig. 3 as log-log plots. When the EGF is slightly larger than unity, linear relations are evident, implying a scaling power law EGF $= (-d\nu/dn)^{-a}$, where $a = 0.53$ to 0.23 depending on the resonance strength and the space-charge tune shift. The *critical tune-ramp rate* is obtained when this linear relationship is extended to intercept the ramp rate axis at EGF $= 1$. We note that at the critical tune-ramp rate, EGF $\lesssim 1.2$. If this EGF is tolerable, the critical tune-ramp rate becomes the required minimum rate to cross the resonance. The critical tune-ramp rate is now plotted against the resonance strength in Fig. 4 for both resonances at $6\nu_{x0,z0} = P$. These plots provide a guide for the design of FFAGs in order to avoid excessive emittance growths when systematic 6th-order resonances are crossed. The linear fits need not be in contradiction to similar plots in Ref. [4] for crossing the systematic 4th-order resonance, because the resonance strengths studied here are less than 1/6 of the maximum 4th-order strengths there.
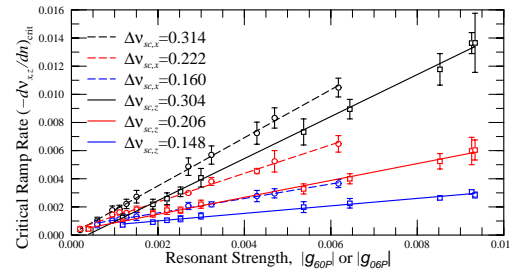
Figure 4: (Color) Critical tune-ramp rate across the systematic 6th-order resonances versus reduced resonance strength $|g_{60P}|$ or $|g_{06P}|$ for various linear space-charge tune shifts or bunch intensities. Dashed and solid lines are linear fits to the data.

4TH-ORDER PARAMETRIC RESONANCE

Octupoles, present either as field errors or as tune-spread provider to Landau damp unwanted transverse instabilities, break the lattice periodicity. To mimic the effects, a single

octupole is added at the D-magnet of the last period of the ring; thus only the resonance $4\nu_{z0} = \ell$ will be studied here.

The potential of the octupole field is $V_4(x, z) = -\frac{B'''}{4!B\rho}\left(x^4 - 6x^2z^2\right)$, where $B\rho$ is the beam rigidity. The terms responsible for the 4th-order resonance can be expressed as $RV_4 \approx -\sum_\ell [|G_{40\ell}|J_x^2 \cos(4\psi_x - \ell\theta + \chi_{40\ell}) + |G_{04\ell}|J_z^2 \cos(4\psi_z - \ell\theta + \chi_{04\ell}) + \cdots]$, where $|G_{mn\ell}|$ and $\chi_{mn\ell}$ are the amplitude and phase of the resonance strength, which can be made dimensionless by introducing $g_{mn\ell} = G_{mn\ell}\epsilon_{\mathrm{rms}}$. Across a thin octupole of length ℓ, the changes in horizontal and vertical divergences are given by $\Delta x' = \frac{1}{6}S_4(x^3 - 3xz^2)$ and $\Delta z' = \frac{1}{6}S_4(z^3 - 3x^2z)$, where $S_4 = B'''\ell/B\rho$ is the octupole strength. For a 1-GeV beam, $S_4 = 50$ m^{-3} corresponds to an octupole with pole-tip field of 0.035 T at radius 5 cm and length $\ell = 1$ m.

Figure 5 shows a sample tracking with 70-turn injection of 4×10^{11} each at bunching factor $B = 0.25$ and bare tunes $\nu_{x0,z0} = 6.95/6.80$, which are then ramped downwards at 0.0005 per turn. The left plots show both the bare (dashes) and space-charge depressed (thick dots) tunes, and the emittance evolution at the octupole strength $S_4 = 20$ m^{-3}. Vertical emittance grows near the $4\nu_{z0} = 27$ resonance at turn 300, which is verified by the vertical phase space plot at turn 270 (top-right). We also see the sum resonance $2\nu_{x0} + 2\nu_{z0} = 27$ at turn 450 and half-integer resonance $2\nu_{z0} = 13$ at turn 800; the latter is verified by the vertical phase space plot at turn 780 (bottom-right). Next come another sum resonance $2\nu_{x0} + 2\nu_{z0} = 26$ at turn 950 and another half-integer resonance $2\nu_{x0} = 13$ at turn 1100. Unlike the systematic resonances studied above, except for the one at $4\nu_{z0} = 27$, there has been severe beam loss when crossing all other resonances. This explains why the octupole strength has been very much limited in this study.

The EGF crossing the resonance $4\nu_{z0} = 27$ is computed for various ranges of the three parameters: resonance strength, tune-ramp rate, and space-charge tune shifts. A
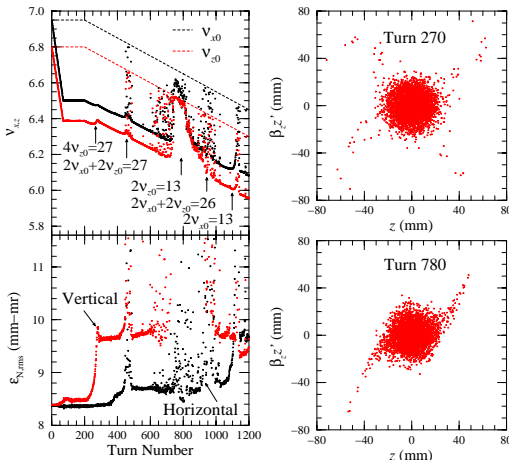
Figure 5: (Color) After 70-turn injection of 4×10^{11} per turn, bare tunes are ramped downwards at 0.0005 per turn (top-left). Emittance growths are seen (bottom-left) while crossing various parametric resonances, usually accompanied by beam loss. Right: vertical phase-space distributions at turns 270 (top) and 780 (bottom), demonstrating the crossing of $4\nu_{z0} = 27$ and $2\nu_{z0} = 13$.
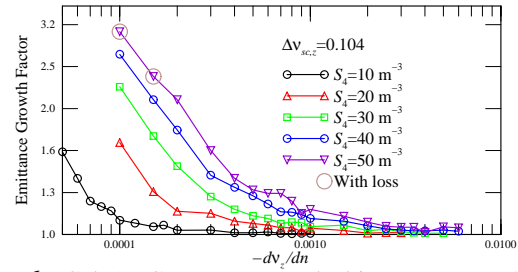
Figure 6: (Color) EGF across octupole driven resonance $4\nu_{x0} = 27$ versus tune-ramp rate for various octupole strengths after 70-turn injection. Linear relationships are evident.

sample result is shown as log-log plots in Fig. 6. Here, power scaling laws are again evident with the power index a varying from -0.35 to -0.65, not by so much as the 6th-order systematic resonance. These linear relationships are extended to intercept the $-d\nu_z/dn$-axis to arrive at the critical tune-ramp rates. In general at these critical tune-ramp rates, EFG is $\lesssim 1.3$. The results are shown in Fig 7, which provides some guidelines for the design of FFAGs. Again linear fits are possible within the error bars.
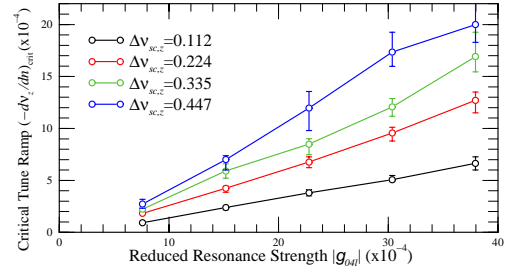
Figure 7: (Color) Critical tune-ramp rate across the octupole driven resonance $4\nu_{z0} = 27$ versus reduced resonance strength $|g_{04\ell}|$ for various bunch intensities.

CONCLUSIONS

Power scaling laws are obtained between the EGF and tune-ramp rate for crossing the space-charge driven systematic 6th-order resonances $6\nu_{x0,z0} = P$ as well as the octupole driven parametric 4th-order resonance $4\nu_{z0} = \ell$. When the resonance strengths are given, they can serve as an estimate to the minimum rate of crossing these resonances in order that the EGF remains tolerable.

The effective space-charge force employed in this investigation is not derivable from a potential. This limits our study concerning the crossing of sum resonances where both transverse spaces are coupled. We are currently working on a better approximation of the space-charge force.

REFERENCES

[1] K.R. Symon, D.W. Kerst, L.W. Jones, L.J. Laslett, and K.M. Terwilliger, Phys. Rev. **103**, 1837 (1956).

[2] C. Johnstone, W. Wan, and A. Garren, PAC'09, p. 3068.

[3] A.G. Ruggiero, Brookhaven Report C-A/AP/#219, 2005.

[4] S.Y. Lee, Phys. Rev. Lett. **97**, 104801 (2008); S.Y. Lee, G. Franchetti, I. Hofmann, F. Wang, and L. Yang, New J. Phys. **8**, 291 (2006).

[5] X. Pang, F. Wang, X. Wang, S.Y. Lee, and K.Y. Ng, Fermilab Report FERMILAB-TM-2395-AD (2007).